

Cellular models in neuroscience

Novak, Andrej

Master's thesis / Diplomski rad

2022

Degree Grantor / Ustanova koja je dodijelila akademski / stručni stupanj: **University of Zagreb, School of Medicine / Sveučilište u Zagrebu, Medicinski fakultet**

Permanent link / Trajna poveznica: <https://um.nsk.hr/um:nbn:hr:105:664497>

Rights / Prava: [In copyright / Zaštićeno autorskim pravom.](#)

Download date / Datum preuzimanja: **2024-05-18**



Repository / Repozitorij:

[Dr Med - University of Zagreb School of Medicine
Digital Repository](#)



UNIVERSITY OF ZAGREB
SCHOOL OF MEDICINE

Andrej Novak

**CELLULAR MODELS IN
NEUROSCIENCE**

Graduation thesis



Zagreb, 2022

This graduate thesis was made at the Laboratory for molecular neurobiology and neurochemistry mentored by prof.dr.sc. Svjetlana Kalanj Bognar and was submitted for evaluation 2022.

Contents

Contents	iii
Summary	1
Acknowledgements	3
Cellular models in neuroscience	4
1. Cellular membrane at rest	4
2. Hodgkin-Huxley model	7
3. Beyond Hodgkin–Huxley model	12
4. Dendrites	14
5. Compartmental models	16
6. The cable equation	18
7. The infinite cable	19
8. Branching points	20
References	27

Summary

In 1952, Alan Hodgkin and Andrew Huxley produced one of the most prolific and significant scientific paper in the history of physiology that was a result of their collaboration that first started in 1939. Their research at the Physiological Laboratory in Cambridge and the Marine Biological Association Laboratory in Plymouth offered key insights into nerve cell excitability. Their legacy includes not only our knowledge of how voltage-gated ion channels influence propagating action potentials, but also the framework for modelling and analyzing ion channel kinetics as they managed to capture the random openings and closings of a plethora of ion channels into just four macroscopic variables; the membrane voltage and three gating variables - much like Fick's law provides a macroscopic description of chemical diffusion in terms of concentration without explicitly considering the underlying Brownian motion of myriad molecules. To this date, it remains one of the greatest illustrations of how phenomenological description combined with mathematical modelling may reveal processes long before they can be detected firsthand (for example by visualization). Their work was awarded a Nobel Prize in Physiology or Medicine in 1963, and served as a basis for numerous other Nobel Prize-winning work. The most notable examples are the work of Erwin Neher and Bert Sakmann's "discoveries concerning the function of single ion channels in cells" ((30) in 1976), and in 2003, Roderick MacKinnon's "structural and mechanistic studies of ion channels" (9). One could argue that this was a starting point for cellular neurophysiology - a broad subfield of neuroscience that studies neurons at the cellular level. In this thesis, we will focus on their results, as well as on a number of different models that arose from it and have sparked the creation of new and attractive research directions of neural models. These types of models are increasingly recognized by both experimentalists and theoreticians as they are opening unique multidisciplinary collaborative research and educational opportunities.

Sažetak

Godine 1952. Alan Hodgkin i Andrew Huxley objavili su jedan od najznačajnijih znanstvenih radova u povijesti fiziologije koji je bio rezultat njihove suradnje započete već 1939. Njihovo istraživanje u Physiological Laboratory u Cambridgeu i Laboratoriju Marine Biological Association Laboratorija u Plymouthu je ponudilo ključne uvide u pobudljivost živčanih stanica. Njihovo nasljeđe ne uključuje samo naše znanje o tome kako naponski vođeni ionski kanali utječu na propagaciju akcijskih potencijala, već i okvir za modeliranje i analizu kinetike ionskih kanala budući da su nasumično otvaranje i zatvaranje mnoštva ionskih kanala uspjeli modelirati samo s četiri makroskopske varijable; napon membrane i tri varijable provođenja - što se može usporediti s Fickovim zakonom koji nudi makroskopski opis difuzije u smislu koncentracije bez eksplicitnog razmatranja temeljnog Brownovog gibanja bezbrojnih molekula. Njihov rad do danas ostaje jedna od najvećih ilustracija kako fenomenološki opis u kombinaciji s matematičkim modeliranjem može otkriti procese mnogo prije nego što se mogu opaziti npr. direktnom vizualizacijom. Njihov je rad nagrađen Nobelovom nagradom za fiziologiju i medicinu 1963. godine i poslužio je kao osnova za brojne druge radove dobitnike Nobelove nagrade. Najznačajniji primjeri su radovi Erwina Nehera i Berta Sakmanna "otkrića funkcija pojedinačnih ionskih kanala u stanicama" (30) objavljenog 1976., te rad iz 2003., koji se bavi "strukturnim i mehaničkim studijama ionskih kanala" autora Rodericka MacKinnona (9). Moglo bi se tvrditi da je to bila početna točka za staničnu neurofiziologiju – široko podpolje neuroznanosti koje proučava neurone na staničnoj razini. U ovom diplomskom radu usredotočit ćemo se na rezultate Hodgkina i Huxleyja, kao i na niz različitih modela koji su iz njih proizašli te potaknuli stvaranje novih i atraktivnih smjerova istraživanja modela neurona. Takvi modeli su sve više prepoznati i od eksperimentalnih i teorijskih znanstvenika jer otvaraju mogućnosti za jedinstvena multidisciplinarna istraživanja i studijske programe.

Acknowledgements

I would like to thank my thesis advisor prof.dr.sc. Svjetlana Kalanj Bognar for her patience, consistent support and guidance. Furthermore, I must express my profound gratitude to my family and friends for providing me with unfailing support and continuous encouragement throughout my years of study. This accomplishment would not have been possible without you. Thank you!

Cellular models in neuroscience

1. Cellular membrane at rest

The lipid bilayer that makes the cell membrane is impermeable to the charged molecules or ions, therefore the movement of several different ion species through various transporters and ion channels inserted in the membrane results in the resting membrane potential (RMP). Out of many different ion species that contribute to the RMP, sodium and potassium have the most impact. This potential is the difference in potentials between the intracellular and the extracellular space, i.e.

$$V_M = V_i - V_o,$$

where V_i and V_o are potentials of the intracellular and extracellular spaces, respectively. Moreover, a variety of negatively charged intracellular proteins and organic phosphates, that do not diffuse freely within lipid bilayers, also play a role. Neurons and muscle cells are excitable, meaning that they can switch from a resting to an aroused state. The resting potential of a typical neuron is around $-65mV$, and is the result of a difference in concentrations of various ions within and outside of the cell. In short, the three most important aspects of RMP are:

- There are significant discrepancies in the ionic content of the extracellular fluid, as it contains high levels of sodium Na^+ and chloride ions Cl^- , whereas the cytoplasm that is abundant with potassium K^+ and a negatively charged proteins. The Na^+/K^+ -ATPase is a major factor in generating the Na^+ and K^+ concentration gradient by pumping three Na^+ ions out of the cell and two K^+ into the cell.

- Cell membrane permeability is selective and the distribution of ions is not uniform. Ions are prevented from freely traversing the plasma membrane by lipid regions, as they can enter or exit a cell only through a membrane channel.
- Ions have varying membrane permeabilities. This indicates that the charges in a cell's passive and active transport systems are not distributed evenly throughout the plasma membrane. Because of their huge size, negatively charged proteins are difficult to permeate the membrane. The inner membrane surface contains more negative charges than the outer surface.

Broadly speaking, there are two types of ion channels: gated and nongated. Nongated channels (also called leaky channels) are constantly open - allowing ions to slowly flow down their concentration gradient. On the other hand, gated channels can open and close, and the probability of their opening is generally dependent on the membrane potential. For example, potassium channels are membrane-spanning tetrameric proteins that show remarkable sensitivity to ion size and valency and conduct around 10^8 K^+ ions per second. The capacity of these channels to conduct and differentiate K^+ from Na^+ at a throughput rate near the diffusion limit is very impressive. Thus, K^+ ions may be promptly released from inside the cell through channels to generate a chain reaction of channel activations that spreads across an axon. At rest, the membrane potential is usually always close to the potassium equilibrium potential due to the membrane's high relative permeability to potassium. Here, the permeability refers to the ease with which ions cross the membrane, and is directly proportional to the total number of open channels for a given ion in the membrane. Conductance, on the other hand, quantifies the ion transport across the membrane. To highlight the importance of ion selectivity, let us mention the recent work by Choi et al (5) that identified recurrent somatic mutations in the selectivity filter of the potassium channel KCNJ5 that are present in certain endocrine tumors linking losses of selectivity to severe hypertension. The current advancements in structural characterization of K^+ channels have been recently discussed by Roux et al (34) where the most relevant findings from experiments, calculations, and a number of fundamental mechanistic problems involving ion conduction and selectivity, have been discussed. Sodium channels will be discussed in the next section. For a more formal discussion, in the context of statistical mechanics, we recommend the book of Gray (14). Most computational approaches for studying ion

channels fall into one of three categories: all-atom molecular dynamics, which is a fully microscopic description with all atoms treated explicitly; Brownian dynamics, in which only the ions are treated explicitly while the solvent, proteins, and lipids are represented implicitly; and approaches based on the Nernst-Planck theory, in which the concentrations of the ions are modelled as a continuum. Here, we follow the later approach to investigate the effects of different ions on the RMP in more detail. By $C(x)$ we denote the concentration of some ionic species, while $V(x)$ is the potential at point x across the membrane. The principal forces that governed this system are the diffusive flux J_d , which yields from the Fick's law of diffusion, and the electric drift J_r that is modelled by the microscopic version of the Ohms law. The total flux across the membrane is then the sum of a diffusive flux and electric drift

$$J = J_d + J_r = -D \frac{\partial C}{\partial x} - \mu z C \frac{\partial V}{\partial x},$$

where D is the diffusion constant, $-\partial V/\partial x$ is the electric field, μ is the mobility, and z denotes the valence of the ion. After using the Einstein's relation to connect the mobility with the diffusion constant, dividing by Avogadro's number N_A to convert the equation into its molar equivalent we get:

$$I = - \left(u z R T \frac{\partial C}{\partial x} + u z^2 F C \frac{\partial V}{\partial x} \right), \quad [1]$$

where $u = \mu/N_A$ is the molar mobility, F is the Faraday constant, and R is the ideal gas constant. Equation [1] is the Nernst-Planck equation. In the equilibrium the net diffusion and electric effects balance, which translates to setting $I = 0$ in the Nernst-Planck equation [1]. After a simple integration, we obtain the Nernst equation for the RMP V_e :

$$V_e = V_i - V_o = - \frac{RT}{zF} \ln \frac{C_i}{C_o} \quad [2]$$

With the assumption that different ions do not interact with each others, and that the total current is the sum of the Na^+ , K^+ and Cl^- currents, we get the Goldman-Hodgkin-Katz equation

$$V_M = - \frac{RT}{F} \ln \left(\frac{P_K [K]_o + P_{Na} [Na]_o + P_{Cl} [Cl]_o}{P_K [K]_i + P_{Na} [Na]_i + P_{Cl} [Cl]_i} \right) \quad [3]$$

where P_j denotes the permeabilities of each of the three ionic species. For a typical neuron at rest, $P_K : P_{Na} : P_{Cl} = 1 : 0.05 : 0.45$. In contrast, approximate relative permeability

values at the peak of a typical neuronal action potential are $P_K : P_{Na} : P_{Cl} = 1 : 12 : 0.45$. Even though this approach has been postulated early in the 20th century, to this day it is a basis for many theoretical models. Recently, Nernst–Planck electro-diffusion theory is discussed in (6) where several techniques for the numerical solution of three-dimensional Nernst–Planck equations are outlined, augmented with numerous examples of ion transport via the protein channels. Moreover, in that contribution, authors extend the concept of ion channel selectivity filters such as electrostatic traps that were not incorporated in the basic Nernst–Planck equation. Such models are more natural and demonstrate phenomena like the ion current saturation with rising bathing solution concentration. In short, these calculations might subsequently be used to assist experimentalists that want to construct altered channels, for example, through site-directed mutagenesis procedures in order to change channel function. For additional details regarding different ion channels and molecular implications of the Nernst–Planck equation, please see (26).

2. Hodgkin-Huxley model

Neuronal activity begins with a brief and localized perturbation in the RMP. This perturbation diminishes with distance from the stimulus, but if it becomes large enough, action potential is produced in the axon membrane. Action potential is an electrical signal that defines a fast and transitory propagating change of the RMP.

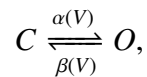
Roughly speaking, we have to model the macroscopic evolution of this perturbation of RMP as this is a cumulative effect of a large number of phenomena that allow its initiation, enhancement, and cessation. To describe the propagation of the potential in the axon, we use the famous cable theory (42). Here, we assume that besides leaky currents, there are K^+ and Na^+ voltage-gated channels spread throughout the axon of a cylindrical shape. We have

$$c_M \frac{\partial V_M}{\partial t} = \frac{a}{2r_L} \frac{\partial^2 V_M}{\partial x^2} - g_K(V_M - E_K) - g_{Na}(V_M - E_{Na}) - g_L(V_M - E_L), \quad [4]$$

where $V_M(x, t)$ is the membrane potential, a is the radius of the cable, g are the conductances of the appropriate channels. The last three terms on the right hand side model the potassium, sodium and the leaky currents, respectively. Using the long-finned *Loligo*

forbesi squid as a model, Hodgkin and Huxley (15) employed a voltage clamp method to experimentally separate the ionic currents and calculated how the conductances change with voltage. This method uses an electrical feedback circuit to regulate the voltage across the membrane of a small region of a nerve cell. Normally, the voltage is regulated to a family of levels that correspond to predefined command patterns, and the current provided or absorbed by the circuit to maintain the voltage at each level is monitored. This current is the same as the ionic current that flows across the membrane in response to the voltage step. In contrast, the current clamp circuit regulates the amplitude of the injected current through a microelectrode while allowing the voltage to fluctuate. A depolarizing current injected across an excitable membrane may be enough to induce an action potential. Changes in membrane voltage produce changes in membrane conductance owing to the opening of populations of ion channels, which subsequently cause changes in sodium and potassium currents across those channels. Whether or not an action potential is created is determined by the balance of these currents. Because TTX and TEA were not available at the time, Hodgkin and Huxley used ion substitutions to address Na^+ and K^+ currents individually. Because the equilibrium potentials were known, the Na^+ and K^+ conductances could be calculated using the Ohms law. Details about the electrical information may be found in the work of Johnston and Wu's (22). It is worth noting that the voltage clamp divides the overall membrane current into ionic and capacitive components. Because capacitive current obeys $I_{cap} = C_M dV_M/dt$, it must be 0 if the membrane potential is being kept constant. Furthermore, by placing a highly conductive axial wire within the fibre, the total current may be rendered spatially uniform; the axon is then said to be space-clamped and the second-order term is then zero. Any variations in current must thus be caused by a leak or the opening and closure of voltage-gated membrane channels.

Hodgkin and Huxley suggested the fundamental model which consists of separate channels with gates that follow first-order kinetics and currents that are carried solely by ions traveling along electrochemical gradients. This may be written as follows:



where C and O correspond to the closed and open states, respectively and functions α and β are called the voltage-dependent transition rate constants. If m is the fraction of open gates, $1 - m$ is the fraction of closed gates, and, according to the law of mass action we get

that the change in number of open gates with time is described with the following equation

$$\frac{dm}{dt} = (\alpha(V)(1 - m) - \beta(V)m) = (m_{\infty}(V) - m)/\tau(V) \quad [5]$$

where

$$m_{\infty}(V) = \frac{\alpha(V)}{\alpha(V) + \beta(V)} \quad \text{and} \quad \tau(V) = \frac{1}{\alpha(V) + \beta(V)}. \quad [6]$$

In order to determine (unknown) functions α and β , there were three degrees of details needed. First, the macroscopic properties of the channel types had to be identified i.e. ionic specificity, maximum conductances, and equilibrium potentials. Second, for each channel type, the number of activation and inactivation gates had to be calculated. Third, equations describing the quantitative voltage dependence of and for each gate type in each channel type had to be developed. In their research, Hodgkin and Huxley determined (unknown) function α and β from the experimental data. A few years later in 1991, Borg-Graham (19) proposed a different approach based on thermodynamics, in which the probability of opening or closing a channel has an exponential dependence on potential

$$\alpha(V) = A \exp(-B \cdot V) \quad \text{and} \quad \beta(V) = C \exp(-D \cdot V), \quad [7]$$

where A, B, C , and D are constants.

The most notable accomplishment of Hodgkin and Huxley, however, was the empirical representation of experimental data in a mathematical model that was the first thorough explanation of a single cell's excitability. They characterized the observed smooth current variations in terms of channels that were either open or closed and gave estimates for the probability of channels being open using a statistical approach. More precisely, they discovered that the conductance change in a voltage clamp experiment had a sigmoid shape during the depolarizing step, and an exponential form during the repolarization (see Figure 1). Moreover, they were aware that single first-order reactions of the sort recommended for the individual channel gates should create exponential curves, but that sigmoid curves would arise from cooperative processes in which numerous first-order reactions are required to occur concurrently. This corresponded to the idea that the channels had several subunits, all of which had to be open at the same time in order for the channel to be open, thus the sigmoid form of the rising curve. On the other hand, just one subunit had to be

closed for the channel to close, resulting in the falling curve's exponential structure. The form of the sigmoid component of the curve in cooperative processes is determined by the number of events involved; the bigger the number of events, the more apparent the inflections on the curve. The precise form of the experimentally observed sigmoid curve indicated that 4 was the best estimate of independent gates inside the K^+ channel. A similar examination of Na^+ conductance curve morphologies indicated that three activation gates and one inactivation gate would best suit the data.

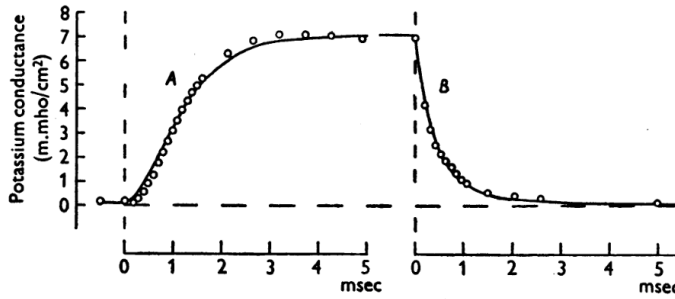


Figure 1: A) increase in potassium conductance due to 25 mV depolarization; B) decline in potassium conductance due to repolarization to RMP. Circles represent a Hodgkin and Huxley experimental measurements (15). The last position of A) corresponds to the initial point of B).

Using the voltage-clamp data, Hodgkin and Huxley derived expressions for the K^+ and Na^+ conductances:

$$g_K = \bar{g}_K n^4, \quad \text{and} \quad g_{Na} = \bar{g}_{Na} m^3 h, \quad [8]$$

where \bar{g}_K and \bar{g}_{Na} are the normalization constant that determine the maximum possible conductance when all the channels are open. The gating variables m, n and h take values between 0 and 1. In the original research, Hodgkin and Huxley thought that a specific amount of charged particles had to move under the effect of the membrane potential in order for K^+ ions to pass. They discovered that introducing n^4 to the onset kinetics produced a satisfactory experimental match to their voltage-clamp data. Similarly, the activation of

the Na^+ current was well suited by three charged particles (m^3), but only one for its inactivation (h). They then used their voltage-clamp data to create equations for calculating n , m , and h at a variety of potentials. These gating variables reflect all of the kinetics' smoothly shifting voltage and time dependency. Thus, the Hodgkin and Huxley paradigm connects ion channels at the microscopic level to currents and action potentials at the macroscopic level.

Following Hodgkin and Huxley in 1960s, others also stipulated that sodium and potassium currents are carried out by specific ion channels. Among others, Chandler and Meves(4), Moore et al (29), Hille (16) and Armstrong (1)), later on used the voltage-clamp technique to further define the functional properties of sodium channels as well as to develop the conceptual models for their function throughout the 1970s. Ion selectivity, saturation, and sodium permeation studies resulted in a thorough model of the sodium channel's ion selectivity filter and its role in sodium selectivity (17). The four-barrier, three-site model, predicted that Na^+ would be partially dehydrated by contact with a high-field-strength site containing a carboxyl side chain at the pore's extracellular end, followed by rehydration in the pore lumen and escape into the intracellular environment. Armstrong (2) in 1973 demonstrated that fast sodium channel inactivation is mediated by protein components on the sodium channel's intracellular surface which were hypothesized to fold into the pore and block it during inactivation. Extensive structure-function studies have revealed the primary functional components of sodium channels. Each domain of the α subunit is composed of two functional modules – a voltage-sensing module consisting of the S1-S4 segments, pore-forming module consisting of the S5 and S6 segments, and the P loop between them. Voltage-dependent activation of the channel depends on gating charges located in the S4 segments. Sodium is selectively conducted through the outer selectivity filter formed by the P loops and the inner pore lined by the S6 segments. After a few milliseconds, sodium channels are inactivated due to a change in the conformation of the intracellular loop connecting domains III and IV. Hille (18) also showed that local anesthetics that act on sodium channels bind to a receptor site in the channel pore which may be accessible by the open activation gate at the intracellular end of the pore. Subsequent research in 1989 revealed that the linker between domains III and IV of the voltage-gated sodium channel subunit was the physical correlate of the inactivation h -gate

(38). For a comprehensive review, please see (7). Furthermore, some neurons exhibit a second pattern of fast inactivation, indicating the presence of an extra gate. Because of a gate that closes the pore and acts as an open-channel blocker, these channels cease transmitting current within milliseconds after depolarization. As discussed by Raman and Bean (46), this gate differs from conventional rapid inactivation in that it reopens with mild repolarization. Blocked channels cannot fast-inactivate or deactivate until they are reopened to remove the blocking particle, further separating this gating mechanism from the original Hodgkin-Huxley formalism.

3. Beyond Hodgkin–Huxley model

The work of Hodgkin and Huxley provided a framework for investigating and analyzing ion channel kinetics that would remain the subject of intense research even to this day. Recently Ori (31), used the Hodgkin-Huxley model to explain how consistent physiological function is maintained in cells, for several homeostatic mechanisms, despite significant variation in critical parameters. Although the whole Hodgkin–Huxley model is very sensitive to variations in its parameters that occur independently, the result is governed by simple structural and kinetic parameters. Structural parameters explain the characteristics of the cell, such as capacitance and ion channel density, whereas, kinetic parameters are those that define how voltage-dependent conductances open and close. When evaluated inside the structural–kinetic plane, the effects of parametric fluctuations on system dynamics seem to be complicated in the high-dimensional representation of the Hodgkin–Huxley model. Slow inactivation, a common activity-dependent property of ionic channels, is shown to be a potent local homeostatic control mechanism that stabilizes excitability in the face of changes in structural and kinetic parameters. This homeostatic process is local, and more importantly, independent of protein synthesis, and functions on many time scales (milliseconds to many minutes). Based on this, one could hypothesize that activity dependence of protein kinetics, at relatively slow time scales as a result of the plurality of protein states, represents a universal automatic and local mechanism of cellular function stability.

Further research generalized the Hodgkin-Huxley model to somata, demonstrating that a variety of Ca^{2+} -dependent currents govern motoneurons and pyramidal cells, and under-

pin the sub-threshold membrane voltage oscillations and resonant features (28). Let us also mention the recent research of Johnston et al (22) that stipulated that dendrites also include a plethora of Ca^{2+} -dependent channels, as we will discuss dendrites in greater detail in the next chapter. These may cause local spikes in dendrites and allow action potentials to be backpropagated into dendrites from the axo-somatic regions. Membrane nonlinearities and action potentials have now permeated our understanding of neurons, forcing us to reassess their functioning principles that were described with only two voltage-dependent currents in the original Hodgkin-Huxley model.

The geometry of excitability may be investigated by reducing the Hodgkin-Huxley model to simple relaxation oscillators which retain the nonlinear nature of the original model but include only two variables: the membrane potential and a slower recovery variable. Namely, the Morris-Lecar model of a neuron (41) is one of such reduced models that is widely known and investigated. The geometric character of the solutions may be revealed via a phase-plane analysis. Phase-plane analysis provides information on the behavior of excitable membranes near their spiking threshold, thus indicating how firing at very low frequencies is possible. Its generalization to higher-dimensional systems with sluggish ionic currents (multi-parameter singular perturbation theory) enabled applied mathematicians (47) to discover the fundamental factors that rise to bursts of firing activity (50). For more details on this approach please see the book of Strogatz (37).

In the last 20 years, the awareness of this rather simplistic view of the action potential grew with the discovery that characteristics of action potentials fluctuate across neuronal types – typically lasting from hundreds of microseconds to several milliseconds – quickly swinging the membrane between hyperpolarized and depolarized states. For example, serotonergic neurons (42) have a distinct electrophysiological profile, which includes regular and spontaneous spiking at a low frequency between 3 and 5 Hz, a constant depolarization in the interspike interval, and wide action potentials lasting between 3 to 6 ms.

Recently, Zhu (53) analyzed the action potential of a single neuron and the synchronous oscillation of a structural neural network by neural energy coding theory energy using the Hodgkin-Huxley model. Their findings suggest that energy consumption is associated with both suprathreshold and subthreshold neural activity, nevertheless, the link between the pattern of brain energy consumption and perceptual cognition is not well understood.

Among other things, they stipulated that prior to firing the action potential, the neuron first saves energy before the peak of the action potential and then consumes it. And, in the power consumption curve, negative energy, or the energy held by the neuron as a result of ATP hydrolysis, accounts for just a trivial part of the overall energy required by the neuron. This neuronal work mechanism may explain the physiological phenomena in which blood flow increases by about 31% but oxygen consumption increases by just 6% in stimulation-induced neural activity. This is consistent with prior studies published by Wang (49).

Even today, devising new therapies for dynamic diseases such as epilepsy, Alzheimer's disease, or Parkinson's disease may be challenging. In the context of nonlinear dynamical systems, such diseases can be thought of as a bifurcation caused by a change in the values of one or more regulating parameters. In neurons, the homeostatic balance between global damping and local excitation can be modelled by the Hopf bifurcation, as it governs many spontaneous oscillations. In our case, this is the initiation or cessation of the self-excited oscillation originating from the equilibrium. Xie (52) used a washout filter-aided dynamic feedback controller to govern the onset of Hopf bifurcation in the Hodgkin-Huxley model and showed that one can shift the Hopf bifurcation to a chosen location using the control strategy, regardless of whether the accompanying steady state is stable or unstable. In other words, it is possible to advance or postpone the Hopf bifurcation to prevent it from occurring within a particular range of the applied current.

4. Dendrites

We are now ready to switch focus towards modelling of dendritic trees as they take up the bulk of the overall neuronal membrane area. Besides the physiological perspective, in the remaining sections, we will also include a more thorough mathematical description. Dendrites allow neurons to form connections with thousands of other cells and to conduct many sub-threshold postsynaptic potentials to the soma that sums these inputs and determines whether the neuron will fire an action potential. In terms of theoretical neurophysiology, mathematical modelling of the integration of synaptic excitation and inhibition, at the neuronal level, allows us to investigate the interactions between several neurons as well as the vast populations of neurons. One could hypothesize that Wilfrid Rall was the

first one to establish the basics for the modern models of the dendritic trees. In his work with the membrane time constant of motoneurons in the cat spinal cord in 1957 he emphasized the significance of dendritic cable characteristics. During the 1970s, cable models were used to model experimental findings that were successfully verified in many laboratories worldwide. Dendrites were once assumed to be passive, with constant conductances and currents; nevertheless, it is now known that dendrites can have active voltage-gated channels, which can have a significant impact on the neuron's firing characteristics and its response to synaptic inputs. When it comes to signal propagation, dendrites function like electrical lines with some insulation properties that would transform an excitatory post-synaptic potential that starts in the dendrite into a much smaller and wider signal by the time it reaches the soma.

Despite the fact that dendrites are densely endowed with voltage-dependent ionic currents, it's imperative to remember that the passive features of the dendritic tree provide the backbone for electrical signalling. The threshold for initiation of a dendritic spike is determined in part by sodium channel availability, but perhaps even more so by the passive load of the surrounding dendrites which determines how much of the input current depolarizes the membrane and how much flows axially toward other dendritic regions (25). Furthermore, if several inputs meet in time and space the resulting interaction will be nonlinear because dendritic synaptic inputs not only inject current but also affect the local membrane conductance to particular ions. Back in 1967, Rall (45) used a mathematical model to describe a case when two excitatory signals are activated simultaneously at a short distance and concluded that each signal depolarizes the membrane and decreases the driving power for the other input, resulting in a response that is less than the sum of the individual responses. Another interesting feature is the shunting inhibition which is a type of nonlinear inhibition that alters the membrane's overall conductance but does not result in a voltage change when activated on its own. Mathematically, we could explain this as lowering the cell's input resistance, which reduces the voltage response to excitatory current (12; 3). Rall also discovered that when excitatory and inhibitory inputs on distinct dendritic branches are far spaced, the inputs will tend to accumulate linearly at the soma. On the other hand, when the excitatory and inhibitory inputs are close together, the inhibition can cause the excitatory input to "shunt" in a highly nonlinear manner. Recently, Liu

(23) experimentally showed that such an inhibition may be localized to a single dendritic branch.

Over the course of the last twenty years, the existence of excitable ionic currents in the dendrites has been shown to promote dendritic action potentials that propagate from the soma to the dendrites (33; 36). A single backpropagating action potential can generate slow dendritic voltage-gated ionic currents, which then flow back towards the initiation zone, resulting in additional action potentials. As a result of its interaction with the dendrites, the somatic action potential might cause a burst under favorable conditions (see (51)). Moreover, many studies suggest that the interaction between the soma and dendrites may be described by a simplified two-compartment model of the neuron. In this case, the coupling coefficient between the two compartments plays a crucial role. The distribution and characteristics of dendritic voltage-gated channels, as well as synaptic activity and plasticity, govern this connection, implying that neuronal firing patterns can thus be altered simply by modifying dendritic characteristics (27; 8; 48). This is still the subject of an active research as the traditional views of dendrites are evolving.

5. Compartmental models

In the approach, the dendritic tree is divided into compartments that are then connected as follows. The parameters of each compartment are assumed to be isopotential and spatially homogeneous. Rather than occurring within compartments, differences in voltage and nonuniformity in membrane parameters, such as diameter, occur between them. We will not describe the interactions between the soma and dendrites, as that is beyond the scope of this thesis. In order to create an arbitrary model of a dendritic tree, one needs only the length, diameter, and geometrical information that instructs him how to connect the cylinders in the right order.

Following the exposition from (44) for a tree-like structure, the equations are then

$$C_j \frac{dV_j}{dt} = -\frac{V_j}{R_j} + \sum_{k \text{ connected } j} \frac{V_k - V_j}{R_{kj}} + I_j, \quad [9]$$

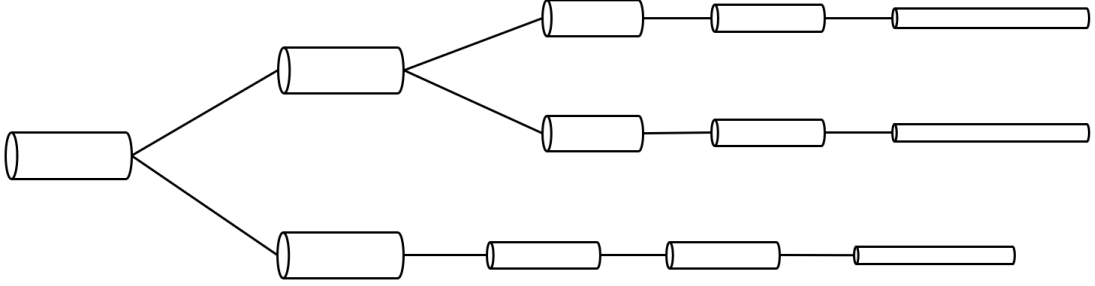


Figure 2: Model of a simple dendritic tree.

where the parameters follow the assumed geometry of the compartments. More preciesly:

- For arbitraty cilinidar the surface area is $A_j = 2\pi a_j L_j$, and the axial resistance factor is $Q_j = L_j/(\pi a_j^2)$.
- The membrane capacitance is $C_j = c_j A_j \times 10^8$, and the membrane resistance is $R_j = (r_{Mj}/A_j) \times 10^8$.
- The coupling resistance between two compartments with indexes j and k is $R_{jk} = \frac{r_L}{2}(Q_j + Q_k) \times 10^4$.

The conversion factors 10^8 and 10^4 are used to scale micrometers to centimeters. In real-world applications, one could take for example one compartment measuring $200\mu m$ in length and $30\mu m$ in radius and second compartment measuring $20\mu m$ in length and $20\mu m$ in radius. This yields $R_1 = 2.65 \times 10^7$, $C_1 = 3.77 \times 10^{-10} F$, for the first compartment and, $R_2 = 3.98 \times 10^8$, $C_2 = 2.52 \times 10^{11} F$, and $R_{long} = 4.34 \times 10^4$, for the second compartment.

Let us remark the reciprocal of the area ratios is the same as the ratio of coupling strengths, revealing that the larger compartment has a considerably bigger impact on the smaller compartment than the smaller compartment does on the larger compartment. In most compartmental models, the usual units for capacitance, conductance, and applied current are microfarads per square centimeter, millisiemens per square centimeter, and microampere per square centimeter, respectively. Experimental scientists usually only know the overall current injected (typically on the order of 1 nA), and not the current density.

6. The cable equation

In many applications, dendrites and axons are treated as continuous media rather than a series of discrete compartments. In the previous sections, we have mentioned the cable equation for a simple cable with a constant radius over the length of the wire. Now, we will extend that approach to more generic geometries by passing to the limit i.e. we will consider the situation when the number of compartments in an approximation approaches infinity so that the length of each compartment becomes infinitesimally small. Let us assume that the circular cable of diameter $d(x)$ is defined on a interval $(0, l)$ and that it consists of n segments of length h . Then each segment has surface area $A_j = \pi d_j h$, $d_j = d(jh)$ and a crossectional area $\pi d_j^2/4$. The equation for voltage then satisfies

$$c_M A_j \frac{dV_j}{dt} = -\frac{V_j}{r_M/A_j} + \frac{V_{j+1} - V_j}{4r_L h/(\pi d_{j+1}^2)} + \frac{V_{j-1} - V_j}{4r_L h/(\pi d_j^2)}. \quad [10]$$

If we divide the previous equation by h and let $h \rightarrow 0$, we obtain the cable equation

$$c_M \frac{dV}{dt} = -\frac{V}{r_M} + \frac{1}{4r_L d(x)} \frac{\partial}{\partial x} \left(d^2(x) \frac{\partial V}{\partial x} \right). \quad [11]$$

In a special case where $d(x) = d$ is a constant, we obtain a linear cable equation

$$\tau \frac{dV}{dt} = -V + \lambda^2 \frac{\partial^2 V}{\partial x^2}, \quad \lambda = \sqrt{\frac{dr_M}{4r_L}}, \quad [12]$$

where λ is the space constant. This parameter is dependent on the cable geometry since it is dependent on the cable diameter. Moreover, the time constant $\tau = r_M c_M$ is a geometrically independent quantity. For example, if $c_M = 1\mu F/cm^2$, $r_M = 20000\Omega cm^2$, $r_L = 100\Omega cm$, and the cable diameter is $2\mu m$, then $\tau = 20ms$ and $\lambda = 1mm$. In this section, we have derived the cable equation and now we are ready to model the appropriate connections between cables in order to describe the branching points. As we will see below, we can differentiate three cases: infinite cable, semi-infinite and finite cable. In the next section, we focus solely on the infinite cable as the semi-infinite and the finite cables are technically more challenging to analyze.

7. The infinite cable

When dealing with an infinite cable we consider the cable equation on the entire real axis ($-\infty < x < \infty$),

$$\tau \frac{dV}{dt}(x, t) + V(x, t) - \lambda^2 \frac{\partial^2 V}{\partial x^2}(x, t) = r_M I(x, t), \quad V(x, 0) = V(x). \quad [13]$$

where $I(x, t)$ is the applied current and $V(x)$ is the initial voltage distribution. Because this equation is linear and defined on the entire real axis, one can use the Fourier transform to get the following:

$$\frac{d\hat{V}}{dt}(k, t) + (1 + \lambda^2 k^2) \hat{V}(k, t) / \tau = r_M \hat{I}(k, t) / \tau, \quad \hat{V}(0) = V_0. \quad [14]$$

This is a first-order linear differential equation with the solution

$$\hat{V}(k, t) = \exp(-(1 + \lambda^2 k^2)t/\tau) \hat{V}_0(k) + (r_M/\tau) \int_0^t \exp\left(-(1 + \lambda^2 k^2)\frac{t-s}{\tau}\right) \hat{I}(k, s) ds. \quad [15]$$

Now by applying the inverse Fourier transform we obtain the solution of the equation [13]

$$V(x, t) = \int_{-\infty}^{\infty} G(x-y) V_0(y) dy + \frac{r_M}{\tau} \int_0^t \int_{-\infty}^{\infty} G(x-y, t-s) I(y, s) dy ds, \quad [16]$$

where

$$G(x, t) = \frac{1}{\sqrt{4\pi\lambda^2 t/\tau}} \exp\left(-\frac{t}{\tau}\right) \exp\left(-\frac{x^2}{4\lambda^2 t/\tau}\right). \quad [17]$$

To further illustrate this model, let us assume that $V_0(x) = 0$ and that $I(x, t) = I_0 \delta(x) \delta(t)$ is a small perturbation from the RMP. The solution in this case is

$$V(x, t) = \frac{1}{\tau \lambda \sqrt{4\pi t/\tau}} \exp\left(-\frac{\tau x^2}{4\lambda^2 t}\right) \exp\left(-\frac{t}{\tau}\right). \quad [18]$$

After some simple calculation one can see that at each spatial location x , this function reaches its maximum at $t^*(x) \approx \tau x^2 / 4\lambda^2$, meaning that the solution V is rapidly decaying, if x is large enough. Next, we comment the remaining cases i.e. the semi-infinite and finite cables as well as the different types of boundary conditions that are imposed on them.

- In the case where we do not allow any current flow at $x = 0$ (sealed end), therefore longitudinal current $I_L = 0$, we impose Neumann boundary condition $\frac{\partial V}{\partial x}(0) = 0$.

- If we inject current of magnitude $I(t)$ at the $x = 0$ we have $\frac{\partial V}{\partial x}(0) \frac{4r_L}{\pi d^2} I(t)$.

As discussed before, the steady state equation $0 = -V + \lambda^2 V_{xx}$ has the solution

$$V(x, t) = A_1 \exp(-x/\lambda) + A_2 \exp(-x/\lambda), \quad [19]$$

where constants A_1 and A_2 are determined by the type of the boundary condition. In the case of a semi-infinite cable we have that $0 < x < \infty$ with the current I_0 being injected at $x = 0$. Because the solution is of the form $V(x) = A \exp(-x/\lambda)$ and we inject longitudinal current $I_0 = -(\pi d^2/4r_L)dV/dx$, we find that

$$A = \frac{4\lambda I_0 r_L}{\pi d^2}.$$

Input resistance of a cable for semi-infinite cable is

$$R_{inp} = V(0)/I(0) = \frac{4\lambda r_L}{\pi d^2} = \frac{2\sqrt{r_M r_L}}{\pi d^{3/2}}.$$

We note that the basic idea for the mathematical modelling of the semi-finite and finite cable is the same, even though, it is far more technically challenging and therefore is omitted from this thesis. For more details on finite cables, please see Chapter 2.4. in the book of Ermentrout (11) or Chapter 5 in the book of Segev (35).

8. Branching points

In reality, besides individual branches that are modelled by finite and infinite cables, neurons have multi-branched structures that we are going to model in this section. We approach this problem by discussing a Rall model for dendrites applied to the simple geometry depicted in Figure 3. Here, d_0, d_1, d_2 and $\lambda_0, \lambda_1, \lambda_2$ are diameters and space constants of the cables, respectively.

Let $x = x_1$ be the branching point, if we assume that the physical properties of the cable are the same, by Kirchoffs law we obtain

$$\frac{\pi d_0^2}{4r_L} V'_0(x_1) = \frac{\pi d_1^2}{4r_L} V'_1(x_1) + \frac{\pi d_2^2}{4r_L} V'_2(x_1). \quad [20]$$

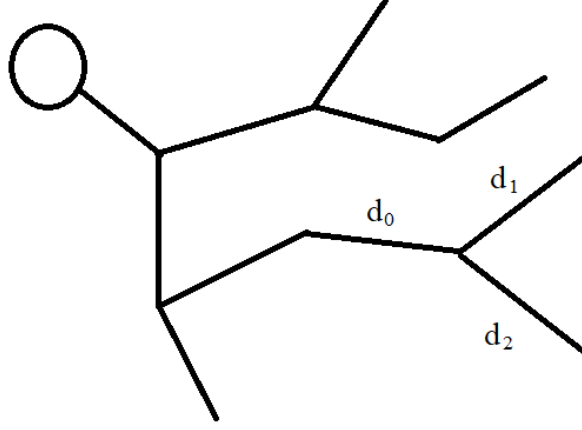


Figure 3: Model of a simple dendritic tree.

Because $V_0 = V_0(x_1) = V_1(x_1) = V_2(x_1)$ it holds

$$V_1(x) = V_0 \exp(-(x - x_1)/\lambda_1) \quad \text{and} \quad V_2(x) = V_0 \exp(-(x - x_1)/\lambda_2), \quad [21]$$

for $x > x_1$. For a membrane potential V_e , let us now extend branch d_0 to the infinity, i.e.,

$$V_e(x) = V_0 \exp(-(x - x_1)/\lambda_0). \quad [22]$$

Substituting these into equation [20] and using the approximation $\lambda_j \approx \sqrt{d_j}$ we notice that all three cables d_0 , d_1 , and d_2 may be collapsed into a single semi-infinite cable (equivalent cylinder) of diameter d_0 where

$$d_0^{\frac{3}{2}} = d_1^{\frac{3}{2}} + d_2^{\frac{3}{2}}. \quad [23]$$

Rall was the first to discover this and offered a recursive strategy to solve a complicated structure starting at the ends. The previous reasoning could be extended to a general case where d_P is the diameter of the parent, and d_D are the diameters of the daughter dendrites.

$$d_P^{\frac{3}{2}} = \sum d_D^{\frac{3}{2}}. \quad [24]$$

By imposing this condition on every branching point, we could collapse the entire dendritic tree to an analogous semi-infinite cable.

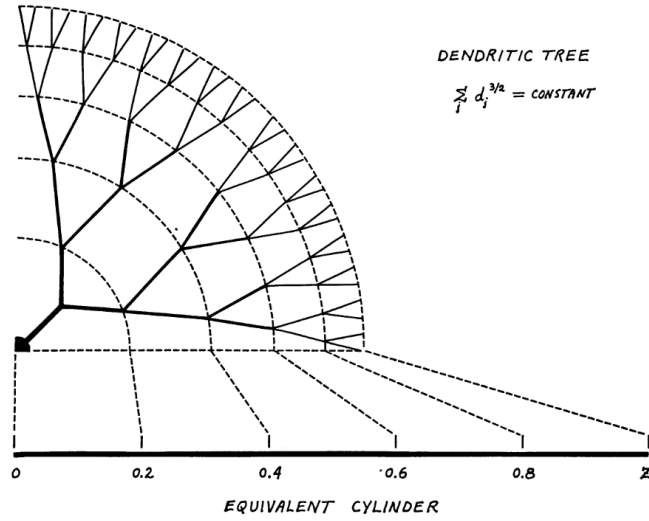


Figure 4: Scheme demonstrating the idea of an equivalent cylinder satisfying the 3/2 rule. Image taken from the original paper of Rall (44).

In this way we have constructed a very useful method for simplifying complicated dendritic tree analyses, never the less, we have to be aware of some constraints that come with it. Besides the 3/2 law [24] that must be met, an additional challenge is identifying the dendritic tree's response to an injected current. If the injection point is d_0 , as modelled in the first example, the corresponding cylinder determines the membrane potential responses at this and daughter dendrites. The equivalent circuit requires that the current be distributed uniformly throughout all daughter dendrites that emanate from the same junction point. The equivalent circuit cannot be used if just one daughter dendrite gets input while the others do not. In the remainder of this section, we will omit the 3/2 rule and consider three semi-infinite cables with a point source of current injection. More precisely, we illustrate this concept on the model shown in Figure 5.

All three membrane potentials $V_i(x)$ satisfy the steady-state equation

$$\lambda_i^2 \frac{\partial^2 V_i}{\partial x^2} - V_i = 0 \quad i = 1, 2, 3, \quad [25]$$

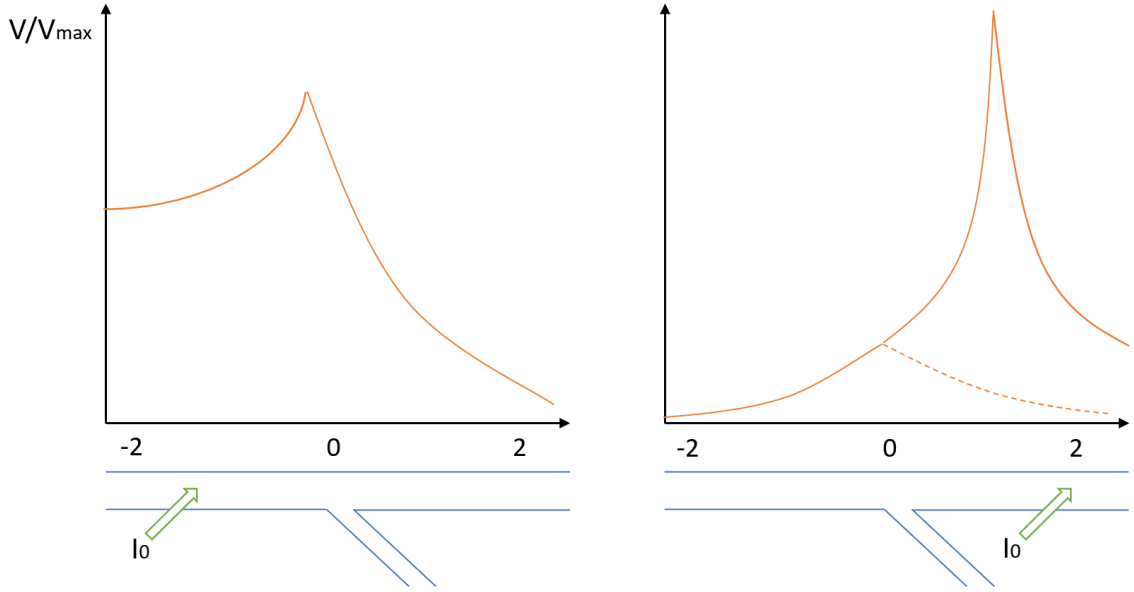


Figure 5: In this figure we can see the dependence of the current injected at two different locations (green arrow) together with the membrane potential along three cables that branch at an isolated junction. (a) The voltage along the thick branch where current is injected is depicted by the solid orange curve for $x < 0$. The potential for both thin wires, which are identical, is shown by the orange curve for $x > 0$. (b) Here we inject the current along one of the narrow wires. The solid orange curve for $x > 0$ represents the potential along the cable where current is injected, whereas the dashed orange curve for $x > 0$ represents the potential along the cable where injection does not occur. Finally, for $x < 0$ with a solid orange curve we depict the potential of the thick cable.

everywhere except at the injection points and the junction at $x = 0$. Here, λ_i is the space constant of the i -th cable.

Let us observe that at the junction point $x = 0$ all three membranes need to be at the same potential

$$V_0(0) = V_1(0) = V_2(0), \quad [26]$$

and the Kirchoff's law must hold, so that

$$\sum d_i^2 \frac{dV_i}{dx}(0) = 0. \quad [27]$$

This current spreads toward or away from the junction point. So the boundary condition at the intersection is given in the terms of the longitudinal current

$$\frac{dV_0}{dx}(y^-) - \frac{dV_0}{dx}(y^+) = \frac{4r_L}{\pi d_0^2} I_0, \quad [28]$$

where I_0 is the electrode current as before, and the terms on the left side of the equation represent the appropriate one-sided derivatives of V_0 . After some purely technical calculations, we arrive to the solution to this problem

$$V_0(x) = \frac{I_0 R_{\lambda_0}}{2} (\exp(-|y - x|/\lambda_0) + (2p_0 - 1) \exp(-(|y| - x)/\lambda_0)), \quad [29]$$

$$V_1(x) = p_1 I_0 R_{\lambda_1} \exp(-x/\lambda_1 - |y|/\lambda_0), \quad [30]$$

$$V_2(x) = p_2 I_0 R_{\lambda_2} \exp(-x/\lambda_2 - |y|/\lambda_0), \quad [31]$$

where

$$p_i = \frac{d_i^{3/2}}{d_0^{3/2} + d_1^{3/2} + d_2^{3/2}}, \quad \text{and} \quad R_{\lambda_i} = \frac{4r_L \lambda_i}{\pi d_i^2}, \quad i = 0, 1, 2. \quad [32]$$

$$V_1(x) = p_1 I_0 R_{\lambda_1} \exp(-x/\lambda_1 - |y|/\lambda_0), \quad [33]$$

$$V_2(x) = p_2 I_0 R_{\lambda_2} \exp(-x/\lambda_2 - |y|/\lambda_0), \quad [34]$$

Now, we can conclude that if the injection site is along the thickest dendrite, the possible attenuation along the thin branches is minimal. In contrast to that, if the injection site is located along one of the thinner dendrites, the thick dendrite has a significantly bigger influence on the attenuation between the two thinner branches.

Up to this point, we have investigated passive dendrites with constant conductances and currents. However, the expression of voltage-gated ion channels is an important determinant of the molecular and functional identity of both axonal and dendritic segments. Several studies (39; 10)) have shown an unequal distribution of ion channels and their varied regulation throughout dendrites and axons, which is required for proper synaptic integration and the formation of suitable action potential firing patterns. Further electrophysiological studies extended this approach to somata, demonstrating that a variety of voltage- or Ca^{2+} -dependent currents regulate the firing pattern of motoneurons and pyramidal cells, as well as the resonance properties. It's been obvious in recent years that

dendrites have a plethora of voltage- or Ca^{2+} -dependent channels (13). Local spikes in dendrites and dendritic spines can result from these, which facilitate action potential back-propagation from the axo-somatic region into the dendrites. For example, sodium channels may be more abundant in the proximal area near the soma. Dendritic generated spikes are believed to play an important part in synaptic integration, although understanding how this happens is difficult. For example, how can a dendritic Na^+ spike impact action potential initiation in the axon if it does not spread out of the dendritic branch where it was generated? The most plausible solution to this perplexing issue is that the dendritic spike, although not actively propagating, does send an extra charge to the axon in addition to the charge arriving through synapses alone. Dendritic excitability, in this manner, reduces the number of excitatory synapses necessary to begin action potential firing in the axon. Thus, while individual synapses in the distal dendrites depolarize the axon vary somewhat due to the dendritic filtering explained above, the effect of distant synapses may be amplified when they contribute to the formation of dendritically triggered spikes. The multicompartment technique is a good way to describe neurons with active dendrites. Among others, Pinsky and Rinzel (32) in 1994 created a guinea pig two-compartment model for CA3 hippocampal pyramidal neurons. This work was inspired by Traub's (43) older, and far more complicated model that included 19 compartments. The simplified Pinsky-Rinzel model retained components of the complete model that were deemed to be crucial, and it was capable of duplicating many of the Traub model's fundamental stimulus-response features, most notable, the bursting phenomena that is rarely seen in single-compartment models. In their two-compartment model, Pinsky and Rinzel divided the rapid sodium spiking currents into a proximal, soma-like compartment (denoted by S) and the slower calcium and calcium-mediated currents into a dendrite-like compartment (denoted by D). There are two voltage-dependent currents in the like compartment S: an inward sodium current and an outward delayed-rectifier potassium current. Three voltage-dependent currents exist in compartment D. Namely, a rapid calcium current and two kinds of potassium currents are modelled: a calcium-activated potassium current and a potassium after hyperpolarization current. For proper parameter levels, the model may produce bursting activity. The research of Hodgkin and Huxley provided an appropriate conceptual framework for understanding spike propagation in axons: uniform and saltatory conduction, as well as

the impact of branching and presynaptic inhibition on spike propagation (20). Membrane nonlinearities and action potentials have infiltrated our understanding of neurons, forcing us to rethink their operating principles. The burst is caused by electrotonic interactions between the soma and dendrite, starting with the somatic sodium spike and followed by the considerable coupling current flowing back and forth between each compartment. Because I_{Na} works at lower voltages than I_{Ca} , the leading sodium action potential depolarizes the dendrite, followed by the partial repolarisation of the soma. This results in lowering the dendritic membrane potential and delays the dendritic spike. The dendrite, in turn, sends current into the soma, causing a second somatic spike. In this way, the dendrite may experience a complete I_{Ca} -mediated voltage spike with a fast rise in calcium. The dendritic spike then depolarizes the soma as the calcium dendritic spikes are wider than the somatic spikes. The wide dendritic spike stimulates the soma, causing damped high-frequency spiking. The calcium-dependent potassium current ends the dendritic calcium spike and hence the burst. During dendritic spiking activity, this slowly builds up, as the burst length is mostly influenced by calcium buildup time. Before a somatic action potential may occur, both currents must decrease.

The basic Hodgkin and Huxley model, with its two voltage-dependent currents, cannot account for all of the events seen, but by adding additional ionic currents, adequate models may be built within the same general framework. Hodgkin and Huxley's equations and their generalizations are a useful tool as they compactly and analytically encapsulate extremely nonlinear features possessed by neurons. Moreover, they include crucial properties such as neural excitability, as well as the activation and inactivation of voltage-dependent currents occurring at different time scales. Hodgkin and Huxley's use of the right biophysical degree of abstraction allows for direct experimental evaluation of model parameters as well as the natural expansion of the model to more sophisticated excitable membranes than the squid giant axon. As a result, it is unmistakable that the Hodgkin and Huxley model established the foundation for studying neuronal excitability. The capacity of this model to remain consistent all these years, despite many new discoveries on membrane excitability in axons and dendrites, indicates that it is here to stay.

References

- [1] Armstrong CM. Interaction of tetraethylammonium ion derivatives with the potassium channels of giant axons. *The Journal of general physiology*. 1971 Oct 1;58(4):413-37.
- [2] Armstrong CM, Bezanilla F, Rojas E. Destruction of sodium conductance inactivation in squid axons perfused with pronase. *The Journal of General Physiology*. 1973 Oct 1;62(4):375-91.
- [3] Blomfield S. Arithmetical operations performed by nerve cells. *Brain research*. 1974 Mar 29;69(1):115-24.
- [4] Chandler WK, Meves H. Voltage clamp experiments on internally perfused giant axons. *The Journal of Physiology*. 1965 Oct;180(4):788.
- [5] Choi M, Scholl UI, Yue P, Björklund P, Zhao B, Nelson-Williams C, Ji W, Cho Y, Patel A, Men CJ, Lolis E. K⁺ channel mutations in adrenal aldosterone-producing adenomas and hereditary hypertension. *Science*. 2011 Feb 11;331(6018):768-72.
- [6] Coalson RD, Kurnikova MG. Poisson-Nernst-Planck theory approach to the calculation of current through biological ion channels. *IEEE transactions on nanobioscience*. 2005 Mar 7;4(1):81-93.
- [7] Catterall WA. From ionic currents to molecular mechanisms: the structure and function of voltage-gated sodium channels. *Neuron*. 2000 Apr 1;26(1):13-25.
- [8] Doiron B, Laing C, Longtin A, Maler L. Ghostbursting: a novel neuronal burst mechanism. *Journal of computational neuroscience*. 2002 Jan;12(1):5-25.

- [9] Doyle DA, Cabral JM, Pfuetzner RA, Kuo A, Gulbis JM, Cohen SL, Chait BT, MacKinnon R. The structure of the potassium channel: molecular basis of K⁺ conduction and selectivity. *science*. 1998 Apr 3;280(5360):69-77.
- [10] Dumenieu M, Oule M, Kreutz MR, Lopez-Rojas J. The segregated expression of voltage-gated potassium and sodium channels in neuronal membranes: functional implications and regulatory mechanisms. *Frontiers in cellular neuroscience*. 2017 Apr 24;11:115.
- [11] Ermentrout B, Terman DH. *Mathematical foundations of neuroscience*. New York: springer; 2010 Jul 1.
- [12] Fatt P, Katz B. The electrical properties of crustacean muscle fibres. *The Journal of physiology*. 1953 Apr 28;120(1-2):171.
- [13] Fellous JM, Houweling AR, Modi RH, Rao RP, Tiesinga PH, Sejnowski TJ. Frequency dependence of spike timing reliability in cortical pyramidal cells and interneurons. *Journal of neurophysiology*. 2001 Apr 1;85(4):1782-7.
- [14] Gray CG, Gubbins KE, Joslin CG. *Theory of Molecular Fluids: Volume 2: Applications*. Oxford University Press; 2011 Oct 13.
- [15] Hodgkin AL, Huxley AF. A quantitative description of membrane current and its application to conduction and excitation in nerve. *The Journal of physiology*. 1952 Aug 28;117(4):500.
- [16] Hille B. Pharmacological modifications of the sodium channels of frog nerve. *The Journal of general physiology*. 1968 Feb 1;51(2):199-219.
- [17] Hille B. Ionic selectivity, saturation, and block in sodium channels. A four-barrier model. *The Journal of general physiology*. 1975 Nov;66(5):535-60.
- [18] Hille B. Local anesthetics: Hydrophilic and hydrophobic pathways for the drug-receptor reaction. *The Journal of general physiology*. 1977 Apr;69(4):497-515.
- [19] L.J. Borg-Gram. *Modelling the nonlinear conductances of excitable membranes. Cellular and Molecular Neurobiology: A practical approach*. 1991.

- [20] d'Incamps BL, Meunier C, Zytnicki D, Jami L. Flexible processing of sensory information induced by axo-axonic synapses on afferent fibers. *Journal of Physiology-Paris*. 1999 Sep 1;93(4):369-77.
- [21] Johnston D, Magee JC, Colbert CM, Christie BR. Active properties of neuronal dendrites. *Annual review of neuroscience*. 1996 Mar;19(1):165-86.
- [22] Johnston D, Wu SM. *Foundations of cellular neurophysiology*. MIT press; 1994 Nov 2.
- [23] Liu G. Local structural balance and functional interaction of excitatory and inhibitory synapses in hippocampal dendrites. *Nature neuroscience*. 2004 Apr;7(4):373-9.
- [24] London M, Häusser M. Dendritic computation. *Annu. Rev. Neurosci.* 2005 Jul 21;28:503-32.
- [25] London, Michael, Claude Meunier, and Idan Segev. "Signal transfer in passive dendrites with nonuniform membrane conductance." *Journal of Neuroscience* 19.19 (1999): 8219-8233.
- [26] Maffeo C, Bhattacharya S, Yoo J, Wells D, Aksimentiev A. Modeling and simulation of ion channels. *Chemical reviews*. 2012 Dec 12;112(12):6250-84.
- [27] Magee JC, Johnston D. A synaptically controlled, associative signal for Hebbian plasticity in hippocampal neurons. *Science*. 1997 Jan 10;275(5297):209-13.
- [28] Manor Y, Rinzel J, Segev I, Yarom Y. Low-amplitude oscillations in the inferior olive: a model based on electrical coupling of neurons with heterogeneous channel densities. *Journal of neurophysiology*. 1997 May 1;77(5):2736-52.
- [29] Moore JW, Narahashi T, Shaw TI. An upper limit to the number of sodium channels in nerve membrane? *The Journal of Physiology*. 1967 Jan 1;188(1):99-105.
- [30] Neher E, Sakmann B. Single-channel currents recorded from membrane of denervated frog muscle fibers. *Nature*. 1976 Apr;260(5554):799-802.

- [31] Ori H, Marder E, Marom S. Cellular function given parametric variation in the Hodgkin and Huxley model of excitability. *Proceedings of the National Academy of Sciences*. 2018 Aug 28;115(35):E8211-8.
- [32] Pinsky PF, Rinzel J. Intrinsic and network rhythmogenesis in a reduced Traub model for CA3 neurons. *Journal of computational neuroscience*. 1994 Jun;1(1):39-60.
- [33] Rapp M, Yarom Y, Segev I. Modeling back propagating action potential in weakly excitable dendrites of neocortical pyramidal cells. *Proceedings of the National Academy of Sciences*. 1996 Oct 15;93(21):11985-90.
- [34] Roux B. Ion conduction and selectivity in K. *Annu. Rev. Biophys. Biomol. Struct.* 2005;34:153-71.
- [35] Segev I. Cable and compartmental models of dendritic trees. *The book of genesis* 1998 (pp. 51-77). Springer, New York, NY.
- [36] Stuart G, Schiller J, Sakmann B. Action potential initiation and propagation in rat neocortical pyramidal neurons. *The Journal of physiology*. 1997 Dec;505(3):617-32.
- [37] Strogatz SH. *Nonlinear dynamics and chaos: with applications to physics, biology, chemistry, and engineering*. CRC press; 2018 May 4.
- [38] Stühmer W, Conti F, Suzuki H, Wang X, Noda M, Yahagi N, Kubo H, Numa S. Structural parts involved in activation and inactivation of the sodium channel. *Nature*. 1989 Jun;339(6226):597-603.
- [39] Trimmer JS. Subcellular localization of K⁺ channels in mammalian brain neurons: remarkable precision in the midst of extraordinary complexity. *Neuron*. 2015 Jan 21;85(2):238-56.
- [40] Tuckwell HC, Penington NJ. Computational modeling of spike generation in serotonergic neurons of the dorsal raphe nucleus. *Progress in neurobiology*. 2014 Jul 1;118:59-101.
- [41] Tsumoto K, Kitajima H, Yoshinaga T, Aihara K, Kawakami H. Bifurcations in Morris–Lecar neuron model. *Neurocomputing*. 2006 Jan 1;69(4-6):293-316.

- [42] Tuckwell HC. Introduction to theoretical neurobiology: linear cable theory and dendritic structure. Cambridge University Press; 1988.
- [43] Traub RD, Wong RK, Miles R, Michelson H. A model of a CA3 hippocampal pyramidal neuron incorporating voltage-clamp data on intrinsic conductances. *Journal of neurophysiology*. 1991 Aug 1;66(2):635-50.
- [44] Rall W. Electrophysiology of a dendritic neuron model. *Biophysical journal*. 1962 Mar;2(2 Pt 2):145.
- [45] Rall W. Distinguishing theoretical synaptic potentials computed for different soma-dendritic distributions of synaptic input. *Journal of neurophysiology*. 1967 Sep;30(5):1138-68.
- [46] Raman IM, Bean BP. Inactivation and recovery of sodium currents in cerebellar Purkinje neurons: evidence for two mechanisms. *Biophysical journal*. 2001 Feb 1;80(2):729-37.
- [47] Rinzel J, Ermentrout GB. Analysis of neural excitability and oscillations. *Methods in neuronal modeling*. 1998;2:251-92.
- [48] Vetter P, Roth A, Hausser M. Propagation of action potentials in dendrites depends on dendritic morphology. *Journal of neurophysiology*. 2001 Feb 1;85(2):926-37.
- [49] Wang R, Tsuda I, Zhang Z. A new work mechanism on neuronal activity. *International Journal of Neural Systems*. 2015 May 2;25(03):1450037.
- [50] Wang J, Chen L, Fei X. Analysis and control of the bifurcation of Hodgkin–Huxley model. *Chaos, Solitons & Fractals*. 2007 Jan 1;31(1):247-56.
- [51] Williams SR, Stuart GJ. Mechanisms and consequences of action potential burst firing in rat neocortical pyramidal neurons. *The Journal of physiology*. 1999 Dec 1;521(Pt 2):467.
- [52] Xie Y, Chen L, Kang YM, Aihara K. Controlling the onset of Hopf bifurcation in the Hodgkin-Huxley model. *Physical Review E*. 2008 Jun 26;77(6):061921.

- [53] Zhu Z, Wang R, Zhu F. The energy coding of a structural neural network based on the Hodgkin–Huxley model. *Frontiers in Neuroscience*. 2018 Mar 1;12:122.

Curriculum vitae

I was born on the June 30, 1987 in Dubrovnik, where I finished elementary and high school. Since then my education is as follows:

- 2016–2022 Doctor of Medicine, University of Zagreb, School of Medicine;
- 2011–2017 Ph.D in Mathematics, University of Zagreb, Faculty of Science;
- 2009–2011 MS in Applied Mathematics, University of Zagreb, Faculty of Science;
- 2006–2009 BSc in Mathematics, University of Zagreb, Faculty of Science.

After my studies in mathematics I attended 8 doctoral and postdoctoral schools in applied mathematics and computer science, I was a postdoctoral researcher at the University of Vienna, published 14 scientific and professional papers, and one chapter in the book. I presented my scientific results on many international conferences world-wide. My scientific interest involves mathematical modelling in medicine, theoretical and numerical partial differential equations.